



# A comparison of two micro-beam X-ray emission techniques for actinide elemental distribution in microscopic particles originating from the hydrogen bombs involved in the Palomares (Spain) and Thule (Greenland) accidents

M.C. Jimenez-Ramos<sup>a,b,\*</sup>, M. Eriksson<sup>c</sup>, J. García-López<sup>a</sup>, Y. Ranebo<sup>d,e</sup>, R. García-Tenorio<sup>a,b</sup>, M. Betti<sup>c,d</sup>, E. Holm<sup>a,e</sup>

<sup>a</sup> Centro Nacional de Aceleradores, Avda. Thomas A. Edison, Isla de la Cartuja, 41092-Sevilla, Spain

<sup>b</sup> Applied Nuclear Physics Research Group, University of Seville, Avda. Reina Mercedes, 2, 41012-Sevilla, Spain

<sup>c</sup> IAEA-MEL, 4 Quai Antoine 1er, MC 98000, Monaco

<sup>d</sup> European Commission, Joint Research Centre, Institute for Transuranium Elements, P.O.Box 2340, D-76125, Karlsruhe, Germany

<sup>e</sup> Department of Medical Radiation Physics, Lund University, SE-221 85, Lund, Sweden

## ARTICLE INFO

### Article history:

Received 30 March 2009

Accepted 2 August 2010

Available online 10 August 2010

### Keywords:

$\mu$ -PIXE

$\mu$ -XRF

Hot particle

U/Pu

## ABSTRACT

In order to validate and to gain confidence in two micro-beam techniques: particle induced X-ray emission with nuclear microprobe technique ( $\mu$ -PIXE) and synchrotron radiation induced X-ray fluorescence in a confocal alignment (confocal SR  $\mu$ -XRF) for characterization of microscopic particles containing actinide elements (mixed plutonium and uranium) a comparative study has been performed. Inter-comparison of the two techniques is essential as the X-ray production cross-sections for U and Pu are different for protons and photons and not well defined in the open literature, especially for Pu.

The particles studied consisted of nuclear weapons material, and originate either in the so called Palomares accident in Spain, 1966 or in the Thule accident in Greenland, 1968. In the determination of the average Pu/U mass ratios (not corrected by self-absorption) in the analysed microscopic particles the results from both techniques show a very good agreement. In addition, the suitability of both techniques for the analysis with good resolution (down to a few  $\mu\text{m}$ ) of the Pu/U distribution within the particles has been proved. The set of results obtained through both techniques has allowed gaining important information concerning the characterization of the remaining fissile material in the areas affected by the aircraft accidents. This type of information is essential for long-term impact assessments of contaminated sites.

© 2010 Elsevier B.V. All rights reserved.

## 1. Introduction

During the last few years, important advances have been made in the field of instrumental analytical techniques for characterizing radioactive environmental particles [1]. In particular special efforts have been devoted for the characterization of hot particles disseminated in two totally different environments after aircraft accidents involving nuclear weapons (the Palomares accident, Spain, 1966, and the Thule accident, Greenland, 1968) [2–11]. The results indicate clear similarities between the particles originating from both accidents: in all the particles highly enriched uranium is mixed with weapon-grade plutonium and the U/Pu mass ratios differ between particles originating from the same accident and even differ inside some particles between the surface and central parts.

In a high proportion of the studies carried out on Palomares and/or Thule hot particles the U/Pu distribution was determined utilising micro

X-ray fluorescence ( $\mu$ -XRF) at a synchrotron facility [2,6,8]. This technique has been shown to be powerful for obtaining the U/Pu mass ratio in this kind of particles, and their results have been validated through the application of destructive radiochemical methods. In addition, synchrotron-based  $\mu$ -XRF technique has also been used to characterize hot particles with other origins: e.g., hot particles released to the Irish Sea by the Sellafield reprocessing plant [12], Pu/U particles released in safety test trials [13], and depleted uranium particles [14]. Thanks to the fast development in X-ray optics, confocal  $\mu$ -XRF setups now can be used providing the possibility to analyse small volumes of the sample at a time rather than the fully excited (by the primary X-ray beam) volume in the sample [15]. The difference between the confocal set-up and a classical  $\mu$ -XRF set-up is that an X-ray lens has been placed in front of the fluorescence detector. The fully excited volume is determined by the size of the primary beam impinging on the sample and the sample thickness in the primary beam direction.

On the other hand, the micro particle induced X-ray emission technique ( $\mu$ -PIXE) can be considered potentially as an alternative microanalytical technique to  $\mu$ -XRF for studying actinide element distribution in particles [16]. It is based on the application of the

\* Corresponding author. Centro Nacional de Aceleradores, Avda. Thomas A. Edison, Isla de la Cartuja, 41092-Sevilla, Spain. Tel.: +34 954460553; fax: +34 954460145.

E-mail address: [mcyrj@us.es](mailto:mcyrj@us.es) (M.C. Jimenez-Ramos).

$\mu$ -PIXE technique using a nuclear microprobe coupled to a 3 MV tandem accelerator. This technique, in combination with the simultaneous application of the  $\mu$ -RBS (Rutherford backscattering) technique allows also to obtain information about the (Pu + U) mass percentage in the hot particles and to perform an estimation of the particle density.

As far as the authors know, ion beam analytical (IBA) techniques and particularly the methodology and analytical procedures applied for obtaining the Pu/U mass ratios distribution by  $\mu$ -PIXE as described in García-Lopez et al. [16] have seldom been applied to the characterization of hot particles. Burns et al. [17] have reported the analysis, using a nuclear microprobe, of particles formed during the nuclear weapons trials at Maralinga, but no information about the measuring conditions or the data treatment is contained in their paper.

The main objective of our work has been to compare the results (Pu/U mass ratios) obtained by the application of the  $\mu$ -PIXE and confocal SR  $\mu$ -XRF to microscopic particles containing actinide elements, in order to validate and gain confidence in both micro-beam techniques for the characterization of these type of particles.

In the characterisation of the environmental mixed U/Pu particles, the experimentally obtained U/Pu L alpha ratios have been considered, taking additionally into account both production cross-section and X-ray fluorescence yields for obtaining the so called in this work U/Pu mass ratios. The X-ray production cross-sections for U and Pu are different and not well defined in the open literature, especially for Pu, leading to a need of inter-comparison of the two techniques. No further corrections due to different self-absorption between the U and Pu characteristics X-rays were done due to the impossibility to know the density distribution inside the analysed particles. The densities of these particles are far from be the theoretical densities of U and Pu in their typical chemical bindings, because they consist very much of a porous material filled with cavities making their density much lower and also quite variable inside them. However, taking into account the composition reported in [16] and the size of the analysed particles, the error caused by the different self-absorption of Pu and U can be estimated 5%–10%.

The characterization by microanalytical techniques of Pu/U hot particles released from weapon-grade material on different ecosystems is extremely important from the radioecological point of view, because, detailed information is required on particle characteristics such as size, composition and morphological structure in order to assess their environmental impact. Indeed, these particle characteristics can be very much dependent on the nuclear source as well as the characteristics of the affected ecosystem and can have high influence in particle weathering rates and subsequent mobilization of radionuclides from particles present in soil–water and sediment–water systems [6].

## 2. Materials and methods

### 2.1. Material

Six hot particles recovered from the sediments in two contaminated areas were analysed, four stem from the Thule accident that occurred in Greenland in 1968, where a B-52 bomber carrying four nuclear weapons crashed on the Arctic ice close to the Thule Air Base. There was an (non-nuclear) explosive fire involving the chemical explosives in the bombs, and areas of the ice and land became contaminated with fissile material. Although the area was decontaminated, some contamination remains even today and is under monitoring and surveillance [11,18].

The other two hot particles were recovered also from marine sediments and originate in the Palomares accident that occurred in South east of Spain in 1966, when a B-52 carrying four nuclear weapons collided in mid air during a refuelling operation. As a result of the accident, two bombs experienced non-nuclear detonations after impacting on land, spreading several kilograms of fissile material.

Although the affected terrestrial area was subjected to a clean-up operation, some contamination remains, with a fraction transported into the neighbouring marine area due mainly to seasonal flooding that historically has affected the zone since 1966 (e.g. Gascó and Antón [19]).

All the particles were separated from sediments that were sampled whit sediment cores in the contaminated zones. These sediments were freeze dried before the particles were isolated.

### 2.2. Hot particle separation and localization

Single hot particles were separated from bulk sediment samples using a sampling splitting technique [20] based on the detection of the  $^{241}\text{Am}$  59.5 keV gamma lines, which is present in the weapon material as a daughter radionuclide of the beta emitter  $^{241}\text{Pu}$ . The technique consists in the division of the sediment sample into two halves and in their measurement by gamma-ray spectrometry. After successive division of the samples, starting with some grams, only few grains remain containing the hot particle.

These isolated grains were then attached to an adhesive carbon tape and examined by scanning electron microscopy (SEM) in the backscattered (BSE) and secondary electron (SE) modes. The BSE mode was used to identify the hot particles due to the high contrast found between elements with high and low atomic number, whereas the SE mode gave information about the topography and size of the particles. In addition, the SEM technique coupled with an energy-dispersive X-ray spectrometer (EDX) confirmed that the particles consisted mainly of U and Pu. Detailed SEM studies of such particles are presented elsewhere [4].

Using SEM, the hot particles were identified and localized on the carbon tape, thus facilitating the re-localization of the particle in subsequent  $\mu$ -XRF and  $\mu$ -PIXE experiments.

### 2.3. Confocal X-ray fluorescence microprobe

The confocal XRF measurements were carried out at the FLUO Beamline of the ANKA synchrotron facility (Karlsruhe, Germany) [21]. A monochromator beam with photon energy  $19.1 \pm 0.5$  keV and a photon flux of  $10^{12}$  ph  $\text{s}^{-1}$   $\text{mm}^{-2}$  was focussed by a compound refractive X-ray lens [22] down to beam size of a few micrometers. The photon energy was set in order to obtain ideal focus conditions of the lens and to excite only the  $L_3$  electron shells of Pu and U.

By knife edge scanning of a 5  $\mu\text{m}$  thin Ni/Fe structure (IRMM 301 standard) the beam size was measured to  $3.12 (\pm 0.05) \times 1.20 (\pm 0.05)$   $\mu\text{m}^2$ . The resulting micro-beam had an intensity of about  $4.10^9$  ph  $\text{s}^{-1}$  in the focal spot.

The XRF spectra were obtained in confocal mode by a Si(Li) detector (133 eV FWHM at 5.9 keV) that was placed in a right angle to the incoming beam in order to minimise the elastic scattering. On top of the detector a polycapillary half lens was attached and lined to form a voxel (common name in 3D reconstruction for a unite volume defined in the scan) with the incoming beam, resulting in a voxel with the dimension of  $dx = 18.4$   $\mu\text{m}$ ;  $dy = 3.12$   $\mu\text{m}$ ;  $dz = 1.20$   $\mu\text{m}$ .

Confocal  $\mu$ -XRF enables to perform three dimensional (3D) scans and give 3D Pu/U distributions within the studied sample. Another great advantage of confocal  $\mu$ -XRF scans, giving important information, is that “low” density volumes can be analysed within the sample. In classical  $\mu$ -XRF this is not possible as the fully excited volume of the primary beam is analysed. If there exist heterogeneities in the density (concentrations) of the different elements in this excited volume, most of the fluorescence photons will come from the areas with highest density (concentration) of the element.

We use this approach by comparing U/Pu mass ratios derived from the summed confocal  $\mu$ -XRF spectra's measured in the full particle volume with the measured mean U/Pu mass ratio derived in all confocal measured volumes. In the calculated mean U/Pu mass ratio,

volumes with low density (concentration) have equal weight to affect the mean U/Pu X-ray intensity ratio, as volumes with high density (concentration). The ratio in the high density volumes can be considered as representative for the bulk of the particles. If one would expect that leaching/corrosion processes have been affecting the particles leading to depletion and lower density (concentration) of elements on the surface, the confocal  $\mu$ -XRF technique is ideal to analyse such surfaces as classical  $\mu$ -XRF would fail. By this important observation, helping in the understanding of the geochemical behaviour that these particles have in the environment could be gained.

The U/Pu X-ray intensity ratios were determined from the corrected (detector dead-time and beam intensity)  $L_{\alpha}$  X-ray lines from U and Pu. Elemental maps were produced with a step size of 3–5  $\mu\text{m}$ , in all (x: horizontal, y: depth and z: height) directions and with a data accumulation time of 10–20 s per data point.

The spectra were deconvoluted with the software program called AXIL [23] using non-linear square fitting. The energies and relative intensities of L and M lines series of Pu have been added to the X-ray library of AXIL based on the database of X-ray transition energies published by Deslattes et al. [24]. The Pu/U X-ray intensity ratios were corrected with the photoelectric cross-sections and the fluorescence yield for characteristic  $L_{\alpha 1} + L_{\alpha 2}$  X-ray emissions, in order to gain the Pu/U mass ratios, but were not corrected by the difference in self-absorption between the characteristics X-rays of U and Pu, due to the reasons given in the previous section (unknown and variable density inside the particles). The photoelectric absorption at 19.1 keV photon energy (allowing U and Pu  $L_3$  and higher electron shells to be excited), are 84.1  $\text{cm}^2/\text{g}$  and 77.5  $\text{cm}^2/\text{g}$  for Pu and U respectively [25], while the fluorescence yield for characteristic  $L_{\alpha 1} + L_{\alpha 2}$  X-ray emission are 0.3726 and 0.3569 per vacant  $L_3$  electron of Pu and U respectively [26].

#### 2.4. Micro-PIXE measurements

The  $\mu$ -PIXE technique was applied using the 3 MV tandem accelerator of the National Accelerator Centre (CNA) in Seville, which is described in detail elsewhere [27]. The microprobe focussing system and the data acquisition set-up are based on an Oxford Microbeams end station OM2000 and on the Oxford Microbeams DAQ system [28], respectively.

The samples were irradiated with a 3 MeV proton beam of size between  $3 \times 3 \mu\text{m}^2$  and  $4 \times 4 \mu\text{m}^2$  (depending on the hot particle analysed) and a beam current of 800 pA. A retractable Si(Li) detector (active area 80  $\text{mm}^2$ , resolution 145 eV) placed at  $135^\circ$  was used, together with a Titan amplifier for  $\mu$ -PIXE analysis.

Elemental maps were done in scanning mode using a field of  $50 \times 50 \mu\text{m}^2$  for all the particles, with the exceptions of Thule 371-4 and Thule 97-1 where the fields were  $100 \times 100$  and  $150 \times 150 \mu\text{m}^2$  respectively. Point measurements were also carried out for all the particles and additional summed spectra from selected areas and from the whole particles were analysed.

In order to increase the peak to noise ratio of the U and Pu L X-ray lines, the measurements were performed using a funny filter in front of the Si(Li) detector. In this way, the low energy X-rays from light elements (Si, Ca, Ti, Fe, etc) that are the main constituents of the soil which partially can coat the analysed hot particles were reduced, as well as the presence of the M line signals of U and Pu. The filter consists of a 1 mm thick mylar film with a 1 mm diameter hole in the centre, to let only a small fraction of the low energy photons to go through. This filter also avoids the backscattered protons to reach the detector, which would otherwise increase the electronic noise.

Maps for U and Pu were determined from the intensities of the  $L_{\alpha}$  lines of these two elements. From the single spot analysis as well as the region analysis the Pu/U X-ray intensity ratios were determined.

The PIXE fitting codes known by the authors are lacking of data (such as cross-sections and atomic branching) for elements with

$Z > 92$ . For that reason, the energies and relative intensities of the L line series for Pu were determined using the Evaluated Atomic Data Library (EADL) [29] and the RELAX code [30] (which takes into account all radiative transitions for each atomic L sub-shell, together with the fluorescence yields and Coster–Kronig probabilities) to calculate the emitted spectrum. This information was included in the X-ray library of the WINQXAS program (same fitting code as AXIL described above) which was used to deconvolute the PIXE spectra and to determine the area of the peaks.

Finally, the sub-shell X-ray production cross-sections  $\sigma(L_{\alpha})$  for 3 MeV protons were calculated for U and Pu [31]. The relative Pu/U mass ratio was then calculated from the  $L_{\alpha}$  peak areas by correcting by the corresponding cross-sections. No further self-absorption corrections were performed because the densities of the analysed particles are not known and quite variable inside them.

The penetration of protons at 3 MeV in the particle is about  $10^2 \mu\text{m}$ . With this information and from the RBS spectra obtained during the measurements we can conclude that we can explore the whole particle in depth. However, the dispersion of the beam, in the other directions inside the particle is small, only tens of  $\mu\text{m}$ .

### 3. Results and discussion

In the upper part of Table 1, the obtained SR  $\mu$ -XRF data for the two analysed Palomares hot particles are shown. The left-hand column show the results obtained from the confocal analysis (i.e. the volume (voxel) derived Pu/U mass ratios) while the middle column show the results obtained from the summed spectra of the whole particles.

The voxel derived mass ratios give a better idea about the homogeneity of the particles as volumes (voxels) with relatively low Pu and U concentrations have equal weight to the mean Pu/U mass ratio of the full particle and the variance of this ratio indicate the homogeneity degree. However, for the summed spectra analyses, the volumes with highest concentration will dominate the mean ratio and indicate the average ratio of the particle material (for the summed spectra analysis, the uncertainty is based on the counting statistics of the  $L_{\alpha}$  peaks of Pu and U).

The results compiled in Table 1 should be compared with the obtained ones by  $\mu$ -PIXE in the same particles, which are shown also in the same Table in the right-hand column. The  $\mu$ -PIXE results included in the latter table correspond to the summed spectra of the whole particles, and are in very good agreement with the obtained ones by SR  $\mu$ -XRF.

For the Palomares particles, the Pu/U mass ratio shows a great difference (0.7 vs. 2.2 by  $\mu$ -XRF and 0.7 vs. 2.4 by  $\mu$ -PIXE). This is in line of previous Pu/U mass ratios published in the literature for hot particles originating from this accident. For example, average values of 1.25 and 2.0 for the Pu/U mass ratios were found in two different Palomares hot particles analysed by applying the  $\mu$ -PIXE technique [16], while in another one the Pu/U mass ratio was found to be  $0.8 \pm 0.2$  by applying radiometric techniques after chemical destruction of

**Table 1**

Confocal SR-XRF and  $\mu$ -PIXE derived Pu/U mass ratios in hot particles originating from Palomares and Thule accidents (n is the number of voxels for each particle in the confocal SR-XRF experiments).

Particle ID	Pu/U ratio $\mu$ -XRF (voxel derived)	Pu/U ratio $\mu$ -XRF (summed spectra)	Pu/U ratio $\mu$ -PIXE (summed spectra)
Palo 1	$0.79 \pm 0.08$ (n = 526)	$0.718 \pm 0.001$	$0.72 \pm 0.01$
Palo 2	$2.37 \pm 0.12$ (n = 30)	$2.215 \pm 0.006$	$2.41 \pm 0.09$
Thu 68-1	$0.20 \pm 0.02$ (n = 67)	$0.172 \pm 0.005$	$0.222 \pm 0.005$
Thu 97-1	N.A.	$0.20 \pm 0.01$	$0.17 \pm 0.01$
Thu 975371-4	$0.12 \pm 0.03$ (n = 622)	$0.113 \pm 0.008$	$0.117 \pm 0.007$
Thu 2003-7524	$0.38 \pm 0.33$ (n = 414)	$0.235 \pm 0.002$	$0.268 \pm 0.006$

Uncertainties 1sd.

the particle [10]. These results can indicate either different Pu/U mass ratio distribution inside the fissile material of each bomb, or different Pu/U signature between the two bombs (most of the available Pu/U mass ratio data can be divided in two groups around the values of 0.8 and 2, respectively).

On the other hand, the results obtained by  $\mu$ -XRF for both Palomares particles indicate that the Pu–U mixture within each particle show a high homogeneity (as reflected in the quite low, 5–10% relative uncertainty, in the voxel derived Pu/U mass ratios). This high homogeneity is graphically reflected in Fig. 1, where the voxel derived Pu/U  $L_{\alpha}$  ratio distribution in the hot particle identified as Palo1 is depicted. This figure shows a normal distribution of the Pu/U  $L_{\alpha}$  ratios with low value of the standard deviation (Fig. 1 represents the Pu/U  $L_{\alpha}$  ratios, and not the Pu/U mass ratios. This fact does not affect the conclusion given in this paragraph, because the same correction factor would be applied to each data).

Through  $\mu$ -PIXE analyses performed either in restricted regions or in points of the analysed Palomares particles, the homogeneity of the interior Pu–U mixture has been confirmed. The SEM images of the Palomares hot particles analysed by  $\mu$ -PIXE and information about their size are included in Fig. 2. The results obtained in each of the analysis for the Pu/U mass ratio are compiled in Table 2. In both particles, the deviation from the average Pu/U mass ratio of the results obtained by analysing some spots or some limited regions are quite small, showing a homogenous distribution of both elements (Pu/U) within the particles, and a very good agreement between the values and results obtained through the application of the two different techniques ( $\mu$ -XRF and  $\mu$ -PIXE).

However, the homogeneity observed in the two analysed particles, cannot be extrapolated to all the particles dispersed in the affected area by the Palomares accident. In other words, the possibility that the Pu and U were fused, either as a consequence of the explosion and

subsequent fire or during the production of the fissile material should not be disregarded.

In the bottom part of Table 1, the obtained SR-XRF data for the four analysed Thule hot particles are also shown. The left-hand column of this Table shows the results obtained from the confocal analysis (i.e. the voxel derived Pu/U mass ratios) while the central column shows the results from the summed spectra of the whole particles.

The results obtained by  $\mu$ -PIXE on the same particles, are also shown in Table 1, and were obtained from the summed spectra of the whole particles. The results obtained with both techniques ( $\mu$ -PIXE and  $\mu$ -XRF) from the summed spectra of the whole particles are in good agreement.

For the analysed Thule hot particles, the Pu/U mass ratios (summed spectra) are more consistent between the particles than in the previous case of Palomares particles. These Pu/U average mass ratios range in the interval 0.11–0.24 ( $\mu$ -XRF) or 0.12–0.27 ( $\mu$ -PIXE), and are clearly lower than what was obtained for the Palomares hot particles (see Table 1). This is in agreement with Lind et al. [8], who analyse particles originating from both accidents (but giving only the  $L_{\alpha}$  ratios) and also agrees with previous Pu/U mass ratios published in the literature for hot particles originating in the Thule accident [11]. In fact, by performing  $\mu$ -XRF analyses on a total of four Thule hot particles with a 20  $\mu$ m beam (this large beam provides information about the average ratio in a large volume of the particles), it was found that the Pu- $L_{\alpha}$ /U- $L_{\alpha}$  intensity ratio varied between 0.22 and 0.36 [1,2].

The main difference between the results obtained by  $\mu$ -XRF for Palomares and Thule particles is the homogeneity of the U/Pu mixture in the particle matrix. The homogeneity of the mixture can be studied by confocal  $\mu$ -XRF. The relative uncertainty of the voxel derived ratios in the Thule particles range from 10% to 87%, indicating a heterogeneous mixture of the particle matrix. This is especially true for the particle Thu 2003-7424 which presents the higher standard deviation. As can be observed in Fig. 3, its voxel derived Pu/U  $L_{\alpha}$  peak ratio distribution is not following a normal distribution, presenting a tail characterised by values of the Pu/U  $L_{\alpha}$  peak ratio higher than 0.5. The voxels with the higher values correspond to the surface of the particle. By excluding the ratios higher than 0.5 (75 voxels) originating from the surface of Thu 2003-7524 (with relatively low concentrations of Pu and U), the voxel derived Pu/U mass ratio for the remaining ones (339 voxels)  $0.25 \pm 0.06$  is closer to the Pu/U derived ratio from the summed spectra, obtained both for  $\mu$ -XRF ( $0.235 \pm 0.002$ , see Table 1) or by  $\mu$ -PIXE ( $0.268 \pm 0.006$ , see also Table 1). In addition, it is in agreement with Pu/U mass ratios determined in other Thule particles. After the removal of the surface data, the remaining derived voxel Pu/U mass ratio has a clearly lower standard deviation, indicating that the great majority of the heterogeneity in the Pu–U mixture is present at the surface of the particle.

The Pu/U mass ratio variations on the surface of Thu 2003-7524 particle agree well with SEM/EDX Pu/U analysis performed previously in this particle [4]. Through EDX measurements performed at different points of the particle, surface Pu/U  $L_{\alpha}$  ratios ranging between 0.08 and 1.40 were found.

The heterogeneity in the Pu/U mixture observed by us through  $\mu$ -XRF in some of the analysed Thule hot particles has been observed also in previous work analysing other hot particles from the same accident. This is the case of the study compiled in Eriksson et al. [2] where varying Pu/U mass ratios along the particle was found by analysing one hot particle also by  $\mu$ -XRF with a 2.5  $\mu$ m beam. Internal specific regions with Pu/U ratios as low as 0.05 were found. Based on these data the authors conclude that the particle can originate from different parts of weapons or from different weapons, rather than be due to an effect of leaching, as the regions with “anomalous” values for the Pu/U mass ratios in this particle have been more or less isolated from the aquatic environment. Lind et al. [8] also obtained semiquantitative information of the actinide distribution on Thule hot-particle surfaces, by performing ESEM–EDX line scans. The

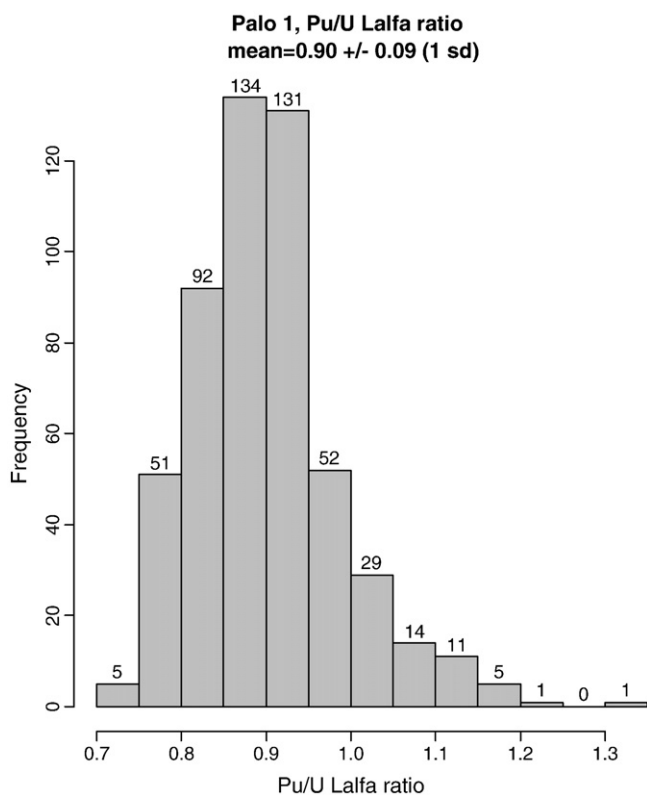


Fig. 1. Palomares hot particle Palo1. Note that the ratios in the figure have not been corrected for ionization cross section nor for the fluorescence yield of Pu and U. The corrected ratios are presented in Table 1.



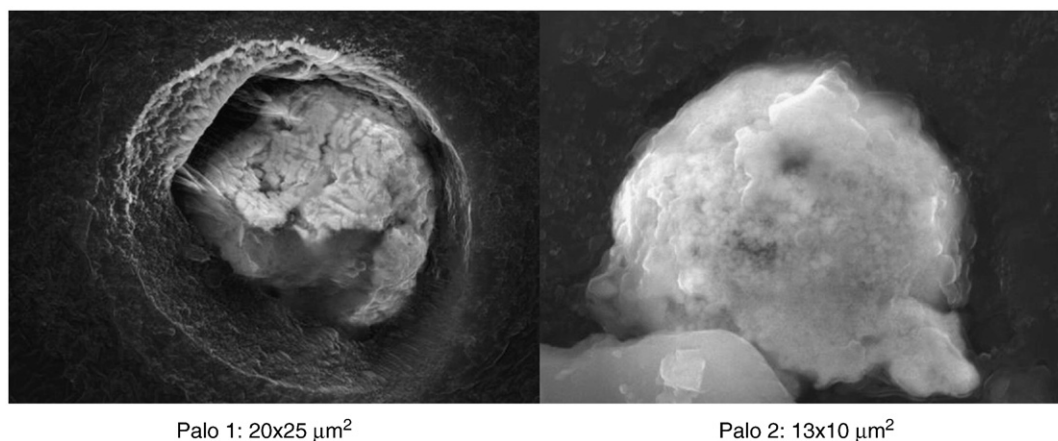


Fig. 2. SEM images of the particles from Palomares.

surface Pu-L<sub>α</sub>/U-L<sub>α</sub> ratio varied between 0.2 and 0.6 with a mean value of 0.3.

Through μ-PIXE analyses performed either in restricted regions or in points of the Thule particles, the previously observed heterogeneity of the Pu–U mixture by μ-XRF has been confirmed. The SEM images of the Thule hot particles analysed by μ-PIXE and information about their size are included in Fig. 4. The results for each Pu/U mass ratio analysis are compiled in the bottom part of Table 2. The results and conclusions obtained through the μ-PIXE analyses of the Thule particles confirm the results and conclusions obtained previously by μ-XRF, reinforcing the idea about the suitability of both techniques for characterization of Pu/U hot particles released through different anthropogenic processes.

In the Thule 68-1 particle, one additional point measurement was performed by μ-PIXE. The Pu/U mass ratio obtained is in excellent agreement with the average Pu/U mass ratio obtained from the whole particle either by μ-XRF or μ-PIXE, as was expected because this particle was the only one showing a high homogeneity in the Pu/U distribution (the relative uncertainty in the average Pu/U derived voxel ratio by μ-XRF was 10%).

In the Thule 975371-4 particle the Pu/U mass ratios determined by performing three punctual μ-PIXE analyses were in the range 0.099–0.149, indicating some degree of heterogeneity in the Pu/U distribu-

tion inside the particle. This heterogeneity was previously deduced from the relative uncertainty in the μ-XRF average Pu/U derived voxel ratio, which in this particle reach the value of 25%.

In the Thule 2003-7524 particle, a total of four limited regions and three points were analysed by μ-PIXE. A detailed study was performed because of its higher degree of heterogeneity in Pu/U distribution revealed in the confocal μ-XRF analysis (the standard deviation of the average Pu/U derived voxel ratio was as high as 87%). The results obtained by μ-PIXE point measurements and mapping analyses confirm the high heterogeneity where values for the Pu/U mass ratios were in a range as ample as 0.182–0.439.

Finally, in the Thule 97-1 particle, which was only analysed by μ-XRF tomography and only the sum-spectra from this scan is available;

**Table 2**  
μ-PIXE derived Pu/U mass ratios in regions and spots of the hot- particles originating from Palomares and Thule accidents.

	Identification	Pu/U ratio
PALO 1	Region a	0.816 ± 0.025
	Region b	0.752 ± 0.081
PALO 2	Point 1	2.592 ± 0.063
	Point 2	2.837 ± 0.125
Thu 68-1	Point 1	0.225 ± 0.004
Thu 97-1	Region 1	0.070 ± 0.005
	Region 2	0.25 ± 0.01
	Region 3	0.26 ± 0.02
	Point 1	0.27 ± 0.01
Thu 975371-4	Point 2	0.064 ± 0.002
	Point 1	0.099 ± 0.003
	Point 2	0.141 ± 0.006
Thu 2003-7524	Point 3	0.149 ± 0.009
	Region 1	0.184 ± 0.013
	Region 2	0.439 ± 0.035
	Region 3	0.250 ± 0.014
	Region 4	0.226 ± 0.013
	Point 1	0.407 ± 0.008
	Point 2	0.422 ± 0.008
Point 3	0.182 ± 0.003	

Uncertainties 1sd.

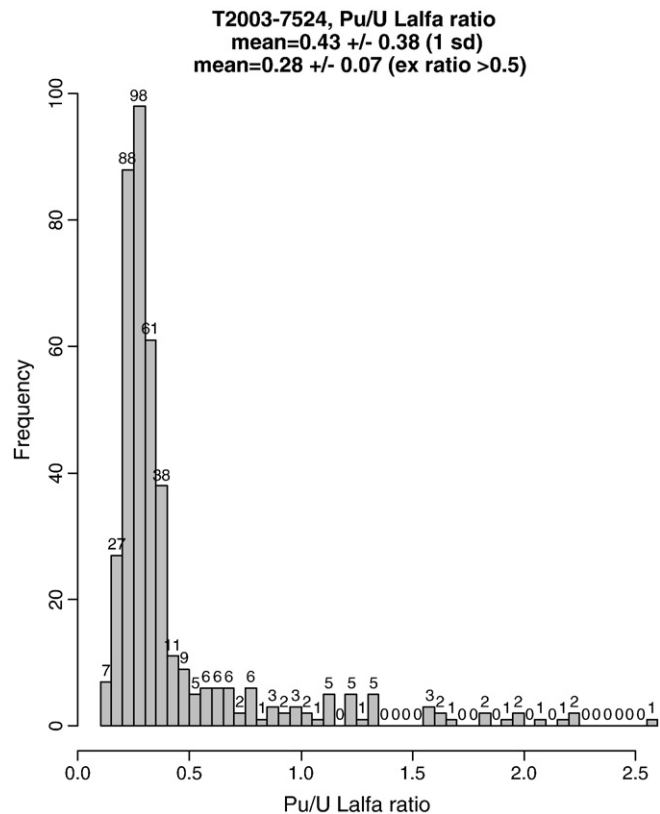


Fig. 3. Thule hot particle Thu 2003-7524. Note that the ratios in the figure have not been corrected for ionization cross section nor for the fluorescence yield of Pu and U. The mean ratios of all voxels are compared with the mean ratio when only the voxels with a ratio lower than 0.5 are considered. The corrected ratios are presented in Table 1.

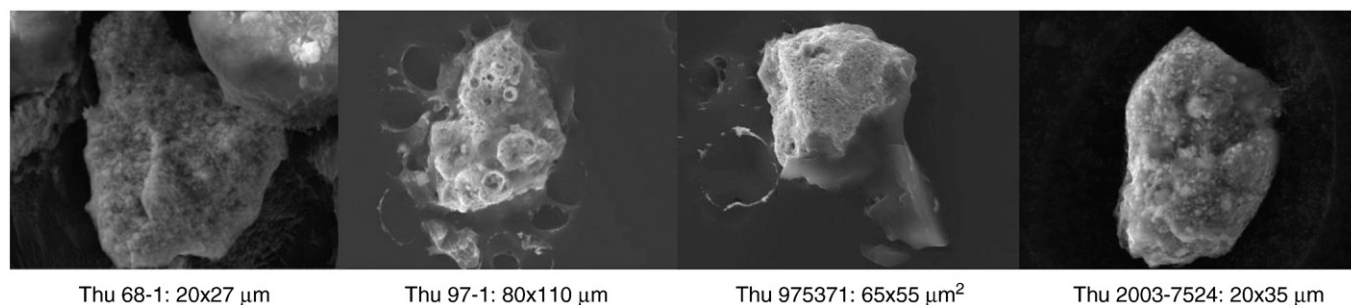


Fig. 4. SEM images of the particles from Thule.

a detailed study was performed by selecting three limited regions and two points for  $\mu$ -PIXE analyses. The obtained results indicate some heterogeneity in the Pu/U ratios within the particle with values ranging in the interval 0.064–0.270. Heterogeneity of this particle has been reported in Eriksson et al. [2], confirming our results. Nevertheless, it is necessary to remark that the lowest values were found in the same zone of the particle (region 1 and point 2, see Fig. 4) while the remainder shows higher and quite uniform Pu/U mass ratio values.

#### 4. Conclusions

The suitability of two microanalytical techniques,  $\mu$ -PIXE and confocal SR  $\mu$ -XRF, for the determination of the average Pu/U mass ratio and the Pu/U mass ratio distribution in hot particles has been evaluated. This evaluation is based on results obtained by applying both techniques to a total of six hot particles released to the environment in two aircraft accidents involving nuclear weapons (Palomares, Spain, 1966 and Thule, Greenland, 1968). A very good agreement was observed between the results obtained by both techniques, including the study with high resolution of the homogeneity in the Pu/U mass ratio distribution within the particles. In addition, the application of both techniques has provided essential information for the characterization of the analysed hot particles which is important for the monitoring of contaminated areas.

#### Acknowledgments

This work has been supported by the Junta de Andalucía Excellence Project RNM 135 (TU-DRAMA – Ultra-sensitive techniques for radionuclides determination in environmental materials). The IAEA is grateful for the support provided to the Marine Environment Laboratories by the Government of the Principality of Monaco. We acknowledge the ANKA Angstromquelle Karlsruhe for the provision of beam time and we would like to thank Dr. Rolf Simon for assistance using FLUO beam line.

#### References

- [1] M. Betti, M. Eriksson, J. Jernstrom, G. Tamborini, Environmental radioactive particles: a new challenge for modern analytical instrumental techniques in support of radioecology, in: M.S. Baxter (Ed.), *Radioactivity in the Environment*, 11, 2008, pp. 355–370.
- [2] M. Eriksson, J. Osan, J. Jernstrom, D. Wegrzynck, R. Simon, E. Chinea-Cano, S. Markowicz, A. Bamford, G. Tamborini, S. Torok, G. Falkenberg, A. Alsecc, H. Dahlgaard, P. Wobrascheck, C. Strel, N. Zoeger, M. Betti, Source term identification of environmental radioactive Pu/U particles by their characterization with non-destructive spectrochemical analytical techniques, *Spectrochim. Acta Part B* 60 (2005) 455–469.
- [3] R. Pöllänen, M.E. Ketterer, S. Lehto, M. Hokkanen, T.K. Ikäheimonen, T. Siiskonen, M. Moring, M.P. Rubio Montero, A. Martin Sanchez, Multi-technique characterization of a nuclear bomb particle from the Palomares accident, *J. Environ. Radioact.* 90 (2006) 15–28.
- [4] Y. Ranebo, M. Eriksson, G. Tamborini, N. Niagolova, O. Bildstein, M. Betti, The use of SIMS and SEM for the characterization of individual particles with a matrix originating from a nuclear weapon, *Microsc. Microanal.* 13 (2007) 179–190.
- [5] M. Moring, T.K. Ikäheimonen, R. Pöllänen, S. Klemola, J. Juhanoja, M. Eriksson, Uranium and plutonium containing particles in a sea sediment sample from Thule, Greenland, *J. Radioanal. Nucl. Chem.* 248 (2001) 623–627.
- [6] O.C. Lind, B. Salbu, K. Janssens, K. Proost, H. Dahlgaard, Characterization of uranium and plutonium containing particles originating from the nuclear weapons accident in Thule, Greenland, 1968, *J. Environ. Radioact.* 81 (2005) 21–32.
- [7] M.C. Jiménez-Ramos, R. García-Tenorio, I. Vioque, G. Manjón, M. García-León, Presence of plutonium contamination in soils from Palomares (Spain), *Environ. Pollut. (Oxford, U.K.)* 142 (2006) 487–492.
- [8] O.C. Lind, B. Salbu, K. Janssens, K. Proost, M. García-León, R. García-Tenorio, Characterization of U/Pu particles originating from the nuclear weapon accidents at Palomares, Spain 1966 and Thule, Greenland, 1968, *Sci. Total Environ.* 376 (2007) 294–305.
- [9] M.C. Jiménez-Ramos, H. Barros, R. García-Tenorio, M.G. León, I. Vioque, G. Manjón, On the presence of enriched amounts of  $^{235}\text{U}$  in hot particles from the terrestrial area affected by the Palomares accident, *Environ. Pollut. (Oxford, U.K.)* 145 (2007) 391–394.
- [10] A. Aragón, A. Espinosa, B. de la Cruz, J.A. Fernández, Characterization of radioactive particles from the Palomares accident, *J. Environ. Radioact.* 99 (2008) 1061–1067.
- [11] M. Eriksson, P. Lindahl, P. Roos, H. Dahlgaard, E. Holm, U. Pu, and Am nuclear signatures of the Thule hydrogen bomb debris, *Environ. Sci. Technol.* 42 (2008) 4717–4722.
- [12] J. Jernstrom, J. Osan, G. Tamborini, S. Torök, R. Simon, G. Falkenberg, A. Alsecc, M. Betti, Non-destructive characterization of low radioactive particles from Iris Sea sediment by micro X-ray synchrotron radiation techniques: micro X-ray fluorescence ( $\mu$ -XRF) and micro X-ray absorption near edge structure ( $\mu$ -XANES) spectroscopy, *J. Anal. At. Spectrom.* 19 (2004) 1428–1433.
- [13] J. Jernstrom, M. Eriksson, R. Simon, G. Tamborini, O. Bildstein, R. Carlos Marquez, S. R. Kehl, T.F. Hamilton, Y. Ranebo, M. Betti, Characterization and source term assessments of radioactive particles from Marshlands islands using non-destructive analytical techniques, *Spectrochim. Acta Part B* 61 (2006) 971–979.
- [14] O.C. Lind, B. Salbu, L. Skipperud, K. Janssens, J. Jaroszewicz, W. De Nolf, Solid state speciation and potential bioavailability of depleted uranium particles from Kosovo and Kuwait, *J. Environ. Radioact.* 100 (2009) 301–307.
- [15] B. Kanngießler, W. Malzer, I. Reiche, A new 3D micro X-ray fluorescence analysis set-up – first archaeometric applications, *Nucl. Instrum. Methods Phys. Res. Sect. B* 211 (2003) 259–264.
- [16] J. García-López, M.C. Jiménez-Ramos, M. García-León, R. García-Tenorio, Characterisation of hot particles remaining in soils from Palomares (Spain) using a nuclear microprobe, *Nucl. Instrum. Methods Phys. Res. Sect. B* 260 (2007) 343–348.
- [17] P.A. Burns, M.B. Cooper, K.H. Lokan, M.J. Wilks, G.A. Williams, Characteristics of plutonium and americium contamination at the former U.K. Atomic Weapons Test Ranges at Maralinga and Emu, *Appl. Radiat. Isot.* 46 (1995) 1099–1107.
- [18] M. Eriksson, On weapons plutonium in the Arctic Environment (Thule, Greenland), Riso-R-1321, Riso National Laboratory, Roskilde, Denmark. Ph. D. Thesis.
- [19] C. Gascó, M.P. Antón, Influence of the submarine orography on the distribution of long-lived radionuclides in the Palomares marine ecosystem, *J. Environ. Radioact.* 34 (1997) 111–125.
- [20] M. Eriksson, K. Ljunggren, C. Hindorf, Plutonium hot-particle separation techniques using real-time digital image systems, *Nucl. Instrum. Methods Phys. Res. Sect. A* 488 (2002) 375–380.
- [21] R. Simon, G. Buth, M. Hagelstein, The X-ray-fluorescence facility at ANKA, Karlsruhe: minimum detection limits and micro probe capabilities, *Nucl. Instrum. Methods Phys. Res. Sect. B* 199 (2003) 554–558.
- [22] V. Nazmov, E. Reznikova, M. Boerner, J. Mohr, V. Saile, A. Snigireva, I. Snigireva, M. Dimichiel, M. Drakopoulos, R. Simon, M. Grigoriev, Refractive lenses fabricated by deep SR lithography and LIGA technology for X-ray energies from 1 keV to 1 MeV, in: T. Warwick (Ed.), *Synchrotron Radiation Instrumentation: 8th International Conference, AIP Conference Proceedings*, Melville, 2004, pp. 752–755.
- [23] B. Vekemans, K. Janssens, L. Vincze, F. Adams, P. Van Espen, Analysis of X-ray spectra by iterative least squares (AXIL): new developments, *X-Ray Spectrom.* 23 (1994) 278–285.
- [24] R.D. Deslattes, E.G. Kessler Jr., P. Indelicato, L. de Billy, E. Lindroth, J. Anton, X-ray transition energies: new approach to a comprehensive evaluation, *Rev. Mod. Phys.* 75 (2003) 35–99.
- [25] M.J. Berger, J.H. Hubbell, S.M. Seltzer, J. Chang, J.S. Coursey, R. Sukumar, D.S. Zucker, XCOM: Photon Cross Section Database version 1.3, National Institute of

- Standards and Technology, Gaithersburg, MD, 2005 Available at: <http://physics.nist.gov/xcom>.
- [26] S.Y.F. Chu, L.P. Ekström, R.B. Firestone, WWW Table of Radioactive Isotopes, , 1999 database version 2/28/1999 from URL <http://nucleardata.nuclear.lu.se/nuclear-data/toi/>.
- [27] J. García-López, F.J. Ager, M. Barbadillo Rank, F.J. Madrigal, M.A. Ontalba, M.A. Respaldiza, M.D. Ynsa, CNA: the first accelerator based IBA facility in Spain, Nucl. Instrum. Methods Phys. Res. Sect. B 161–163 (2000) 1137–1142.
- [28] G.W. Grime, M. Dawson, M. Marsh, I.C. McArthur, F. Watt, The Oxford submicron nuclear microscopy facility, Nucl. Instrum. Methods Phys. Res. Sect. B 54 (1991) 52.
- [29] S.T. Perkins, D.E. Cullen, M.H. Chen, J.H. Hubbell, J. Rathkopf, J. Scofield, Table and Graphs of Atomic Sub-shell and Relaxation Data Derived from the LLNL Evaluated atomic Data Library (EADL), Z = 1–100, UCRL-50400, vol. 30, 1997.
- [30] D.E. Cullen, Program Relax, a Code Designed to Calculate Atomic Relaxation Spectra of X-Rays and Electrons, LLNL, 1992.
- [31] D.D. Cohen, M. Harrigan, At. Data Nucl. Data Tables 34 (1986) 393–414.